Temperature Affects the Supramolecular Structures Resulting from α-Lactalbumin−Lysozyme Interaction

Michaël Nigen,[‡] Thomas Croguennec,[‡] Denis Renard,[§] and Saïd Bouhallab*[,‡]

INRA, Agrocampus Rennes, UMR 1253, Science & Technologie du Lait et de l'Œuf, 65 rue de Saint Brieuc, F-35000 Rennes, France, and INRA, Unité Biopolymères, Interactions, Assemblages, Rue de la Géraudière, BP 71627, F-44000 Nantes, France

Received October 12, 2006; Revised Manuscript Received November 30, 2006

ABSTRACT: The interaction between α-lactalbumin and lysozyme, two globular proteins with highly homologous tertiary structures but opposite electric charges, was investigated. As assessed by isothermal titration calorimetry, lysozyme did not bind to the native form of α-lactalbumin but did interact with calcium-depleted α-lactalbumin (apo α-LA). This interaction leads to the formation of different supramolecular structures depending on the temperature. Heterogeneous, amorphous aggregates are formed at 5 °C, while droplets, coacervate-like structures, exist at 45 °C. The coacervates are formed by equimolar quantities of the two proteins, but their size and number depend on the initial protein molar ratio. These supramolecular structures are found to be stable when the temperature is decreased to 5 °C, while prolonged heating at 45 °C induces the formation of larger coacervates through a coalescence phenomenon. Surprisingly, interplay occurs between aggregates and coacervates when the temperature is increased from 5 to 45 °C. We discuss the results in terms of subtle heat-induced conformational changes in apo α-LA. In conclusion, our results show an association between globular proteins that leads to the formation of a variety of supramolecular structures in a temperature-dependent manner and confirm the primordial role of certain α-lactalbumin unfolding intermediates in protein-driven assembly.

Protein−protein interaction is relevant and important in both medical and food science. These interactions modify the protein structure and unfolding process and may lead to a variety of supramolecular structures. Understanding protein−protein interaction in multiprotein systems is a key factor in controlling the formation of protein aggregates and opening the field of nanostructured protein assemblies. For this purpose, two globular proteins, bovine α-lactalbumin (α-LA) and hen egg white lysozyme (LYS),[1] for which a wealth of information is now available at the molecular level were used. α-LA and LYS are two related proteins of 123 and 129 amino acid residues, respectively, which have amino acid sequences that are ∼40% similar and share a similar three-dimensional structure, including four disulfide bonds (*1*−*3*). These proteins differ particularly in their biological function and their opposite isoelectric points. α-LA is an acidic protein with a pI value near 4−5, while LYS is a basic protein with a pI value of 10.7. Indeed, notable differences among these two proteins reside in their calcium binding properties and their ability to adopt partly folded states or molten globules in acid solutions (*3*).

α-LA, a small monomeric milk protein, consists of two lobes: a large basic α-helical lobe and a small acidic *β*-sheet domain, which are connected by a calcium binding loop (*4*−*8*). The calcium located between the two lobes plays a key role in the structure, functionality, and stability of α-LA; its denaturation temperature is ∼64 °C (*9*). Calcium is particularly coordinated by the *β*-carboxylate group side chains of three aspartic acid residues (*3*, *6*, *10*). Removal of calcium from holo α-LA to generate the apo form destabilizes the protein and decreases its thermal stability due to negative charge−charge repulsions at the calcium binding site (*7*).

LYS is a relatively small secretory protein that catalyzes the hydrolysis of specific kinds of polysaccharides comprising the cell walls of bacteria. It is a basic protein exceptionally abundant in egg white. It is also one of the best characterized and most studied proteins. Its folding−unfolding mechanism has been studied in detail (*11*). The three-dimensional structure of lysozyme is formed by two domains with a first predominantly α-helical domain and a second *β*-sheet domain. By contrast to bovine α-LA, LYS from hen egg white does not contain a specific metal binding site in its structure. LYS is relatively stable, its denaturation temperature being 74 °C (*12*−*14*).

This study constitutes a part of a research program aimed at investigating how food proteins interact and aggregate together under various physicochemical conditions. The potential interaction of LYS with either native α-LA (holo α-LA) or its calcium-depleted form (apo α-LA) was first examined by isothermal titration calorimetry. The detected interaction between LYS and apo α-LA was further explored at different temperatures via characterization of supramolecular structures formed by means of turbidity, optical microscopy, and reverse phase high-performance liquid chromatography. The results revealed that different structures,

* To whom correspondence should be addressed. Telephone: 00 33 (0)223485742. Fax: 0033(0)223485350. E-mail: said.bouhallab@rennes.inra.fr.
‡ INRA, Agrocampus Rennes, UMR 1253.
§ INRA, Unité Biopolymères, Interactions, Assemblages.

[1] Abbreviations: apo α-LA, calcium-depleted α-lactalbumin; LYS, hen egg white lysozyme; rp-HPLC, reverse phase high-performance liquid chromatography; ITC, isothermal titration calorimetry.

10.1021/bi062129c CCC: $37.00
Published on Web 01/09/2007

amorphous aggregates versus droplets, coacervates-like structures, were generated depending on working temperature.

MATERIALS AND METHODS

Reagents. Hen egg white lysozyme (LYS) was purchased from Ovonor and contained 95% LYS and 3% chloride ions. Holo α-LA was purified from bovine whey as reported by Caussin et al. (*15*). The resulting powder contained 95% holo α-LA. Apo α-LA was prepared by dialysis of a solution of holo α-LA against deionized water at pH 3 for 48 h at 4 °C using a dialysis membrane (Spectrum Laboratories) with a nominal cutoff of 6000−8000 Da to remove calcium ions. The pH of the apo α-LA solution was adjusted to pH 7 with 1 M NaOH and then freeze-dried. The calcium content of the apo α-LA powder was analyzed by atomic absorption spectrometry on a SpectrAA 220FS instrument (Varian, Les Ulis, France); the Ca/apo α-LA molar ratio was less than 2%.

Stock solutions of LYS, holo α-LA, and apo α-LA were prepared by solubilization of protein powders in 30 mM Tris-HCl, 15 mM NaCl buffer (pH 7.5). They were filtered through a 0.2 μm membrane before preincubation at the working temperature. The protein concentration was determined by measuring the absorbance at 280 nm using extinction coefficients of 2.01 and 2.64 L g^{-1} cm^{-1} for apo α-LA and LYS, respectively.

Isothermal Titration Calorimetry (ITC). ITC experiments were performed on a VP-ITC microcalorimeter (Microcal, Northampton, MA). Stock solutions of α-LA, apo α-LA, and LYS were diluted in 30 mM Tris-HCl, 15 mM NaCl buffer (pH 7.5) at final concentrations of 0.32, 0.32, and 2.3 mM, respectively. Samples were degassed under vacuum before titration experiments. Measurements were carried out at 5, 25, and 45 °C. The reference cell was filled with deionized water, and the sample cell (1.425 mL) was filled with either an α-LA or an apo α-LA solution. After an equilibration time at the working temperature, apo α-LA was titrated with 29 successive 10 μL injections of LYS. The injection time was 10 s, and the lag time between injections was fixed at 130 or 200 s to allow complete thermodynamic equilibrium. During titrations, the solution in the sample cell was stirred at 300 rpm in the injection syringe to ensure complete mixing of the solution. References were obtained by injecting LYS into a cell containing the buffer solution. Data resulting from the subtraction of reference values (dilution heat) from the sample values were analyzed using MicroCal ORIGIN version 7.0 provided by the manufacturer. For each experiment, the area under each peak was plotted versus the LYS/apo α-LA molar ratio. All experiments were repeated at least three times.

Preparation of the Protein Mixtures. Solutions with different LYS/apo α-LA molar ratios ranging from 0.05 to 2 were prepared from stock solutions of LYS and apo α-LA and kept at a temperature of 5 or 45 °C. Further analyses were performed after equilibration for 30 min at these two temperatures. All prepared protein mixtures contained a constant final apo α-LA concentration of 0.266 mM, except when specified in Results. All the analytical experiments performed below were repeated at least three times.

Optical Microscopy. Structures resulting from the mixing of apo α-LA and LYS at 5 and 45 °C were observed using a phase contrast optical microscope (Olympus BX51TF) equipped with an Olympus DP11 camera. Samples were put between glass slides, and structures were immediately observed at a magnification of 100× at room temperature. The irreversibility of structures formed at 45 °C limits any important change between sampling and microscopic examination.

Particle Size Determination. The size of the structures formed in the mixtures at 45 °C was investigated by laser dynamic light scattering (DLS) using a Malvern HPPS instrument (Malvern zetasizer Nano ZS). Measurements were performed 15 min after the preparation of the samples in a 1 cm path length spectroscopic plastic cell at 45 °C. Before each measurement, solutions were gently stirred. Experimental data were analyzed using the Contin algorithm provided by the manufacturer. Samples with a LYS/apo α-LA molar ratio of >0.2 were diluted 21 times before measurements to avoid detector saturation. Each measurement was performed in duplicate.

Reverse Phase HPLC Analysis. We performed reverse phase separation on a Vydac C_4 column (214TP5215) connected to a HPLC system, consisting of a Waters 2695 separations module, a Waters 2487 dual λ absorbance detector, and Empower (Waters) to acquire, process, and report chromatographic profiles. Milli-Q water containing 1.06‰ (v/v) trifluoroacetic acid as buffer A and an 80:20 (v/v) acetonitrile/Milli-Q water mixture containing 1‰ (v/v) trifluoroacetic acid as buffer B were used for protein elution. The gradient started with 20% buffer B to reach 84% in 22 min. Protein separation was carried out at a flow rate of 0.2 mL/min at 40 °C. Proteins were detected simultaneously at 214 and 280 nm.

Before analysis, samples were centrifuged at 12000*g* for 30 min at 5 or 45 °C. Supernatants were recovered, and pellets were washed with 30 mM Tris-HCl, 15 mM NaCl buffer (pH 7.5) and then dissolved in a buffer A volume equivalent to the initial volume. Samples were diluted 100 times in buffer A before injection.

Turbidity Measurement. Turbidity was measured on a 6505 UV−vis spectrophotometer (Jenway, Chelles, France) equipped with a temperature-controlled cell connected to a circulating water bath. Optical density (OD) was measured 30, 90, and 150 min after the preparation of the samples at 600 nm and 45 °C. Before each measurement, solutions were gently stirred. Sample turbidity (τ) was determined using the relationship $\tau = (2.303\mathrm{OD})/l$, where OD is the optical density of the sample and l is the light path length in the cell (1 cm).

Solutions with a LYS/apo α-LA molar ratio higher than 0.2 were diluted five times before turbidity measurements. For samples with a lower protein molar ratio, measurements were performed on undiluted samples.

RESULTS

Isothermal Titration Calorimetry (ITC). When native holo α-LA was titrated with LYS, no signal was detected from ITC (results not shown). On the other hand, when calcium-depleted α-LA, i.e., apo α-LA, was used, raw data displayed large amplitude responses at all the temperatures that were studied. The heat flow versus time profiles resulting from the titration of apo α-LA with LYS at various temperatures

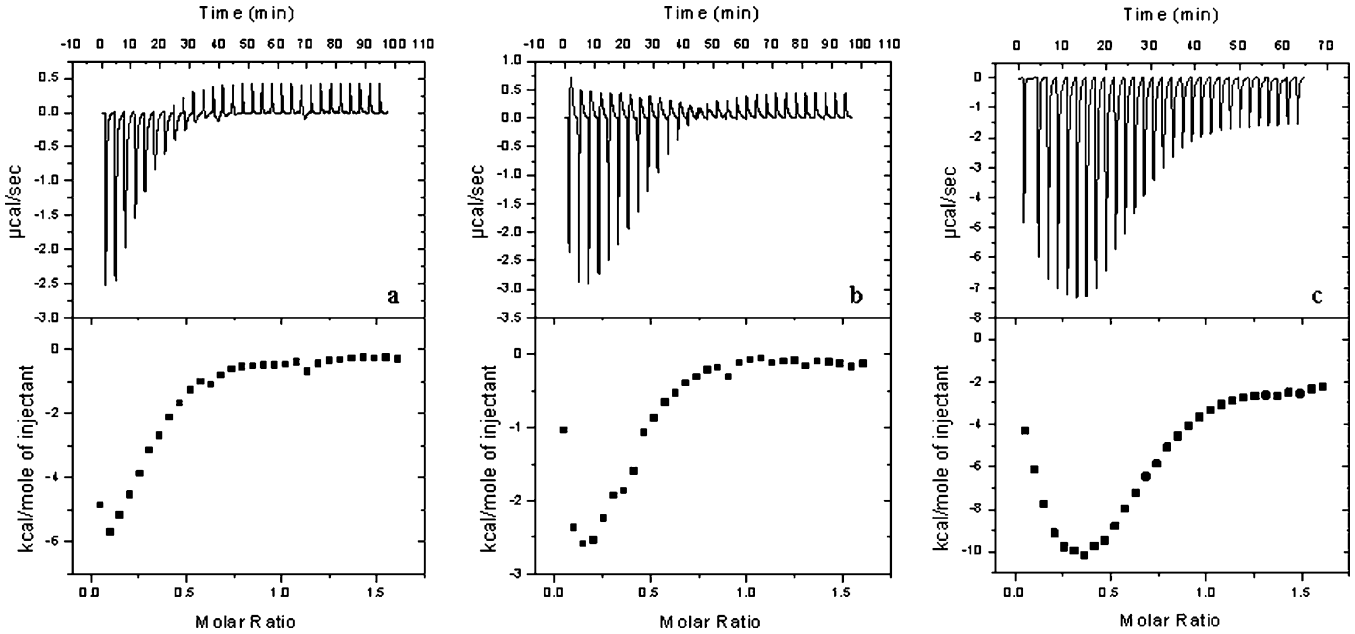

FIGURE 1: Microcalorimetric titration of apo α-LA with LYS in 30 mM Tris-HCl, 15 mM NaCl buffer (pH 7.5) at 5 (a), 25 (b), and 45 °C (c). Top panels represent the raw heat signal for the titration of apo α-lactalbumin (0.32 mM) with 10 μL increments of 2.3 mM lysozyme. Bottom panels represent the area under each peak integrated and plotted against the LYS/apo α-LA molar ratio.

are shown in Figure 1 (top panels). The area under each peak represented the heat exchange within the system after each injection. At 5 °C (Figure 1a), the injection profiles of LYS in the sample cell containing apo α-LA were exothermic and decreased regularly to become endothermic and constant after the 10th injection (corresponding to a LYS/apo α-LA molar ratio of 0.5). At 25 °C (Figure 1b), the first 13 injection peaks exhibited both an exothermic and endothermic contribution while an endothermic signal was obtained for subsequent injections. During the first injections, the interaction between LYS and apo α-LA exhibited a complex behavior. The endothermic signal after the 10th and 14th injections at 5 and 25 °C, respectively, corresponded to the dilution signal of LYS in the sample cell as assessed in a reference experiment. At 45 °C (Figure 1c), an exothermic signal was obtained for all injections. The signal corresponding to the dilution of LYS, also endothermic at 45 °C, was masked by other phenomena.

Titration curves of LYS−apo α-LA interaction, shown in Figure 1 (bottom panels), are obtained by integration of the isotherm peaks and subtraction of the heats of dilution of LYS into buffer solution. The resulting curves at 5, 25, and 45 °C showed that the complexation between LYS and apo α-LA was exothermic at all tested temperatures. The first injection was not taken into account for analysis. At 5 °C (Figure 1a), the energy released in the sample cell decreased as the molar ratio increased. The saturation of apo α-LA with LYS was reached at a molar ratio of ∼1. At 45 °C (Figure 1c), the shape of the titration curve showed two distinct thermodynamic events during the interaction between apo α-LA and LYS. (i) the heat released increased first from 6.15 to 10.17 kcal/mol of LYS injected for molar ratios ranging from 0.10 to 0.36, respectively. (ii) The heat released following LYS injection decreased then from 10.17 to 2.8 kcal/mol to reach a plateau value for a molar ratio of >1.25. At 25 °C (Figure 1b), the heat released increased slightly from 2.4 (second injection) to 2.6 kcal/mol of LYS injected (third injection) and then decreased to reach saturation at a molar ratio of ∼1. The shape of the titration curves obtained at 25 °C was similar to that obtained at 45 °C with two successive events, the first event being, however, shorter at 25 °C.

Whatever the temperature, the shapes of titration curves were rather complex. As a consequence, fitting experimental data to an integrated binding isotherm could not be performed and no interaction parameters were determined. However, the temperature dependence of the interaction between apo α-LA and LYS was evidenced from ITC experiments.

Characterization of the Supramolecular Structures. During ITC experiments, we noted the formation of a whitish precipitate at the end of titration, the visual aspect of which depended on the working temperature. The precipitate obtained at 5 °C looked more compact, fluffy, and dense than that obtained at 45 °C. The aim of the following sections was to better characterize the formed precipitates following formation of the LYS−apo α-LA complex at 5 and 45 °C.

Optical Microscopy. Phase contrast micrographs obtained at 5 and 45 °C for different LYS/apo α-LA molar ratios, ranging from 0.05 to 1.5, are shown in Figure 2. At 5 °C (Figure 2a−d), aggregates with irregular shape were observed for all the protein molar ratios that were studied. From theses micrographs, aggregate sizes were estimated to range from 1−2 to 20−50 μm. Small aggregates were observed whatever molar ratios were studied, whereas numerous larger aggregates were observed for higher molar ratios (Figure 2b−d). Consequently, aggregates in solution were polydisperse in size for each molar ratio. Moreover, the number and average size of aggregates seemed to increase with increasing LYS/apo α-LA molar ratios. According to the polydispersity in the aggregates size observed by optical microscopy, the aggregates were not further analyzed by dynamic light scattering.

At 45 °C, the particles looked completely different (Figure 2e−h). Coacervate-like structures, with spherical and regular

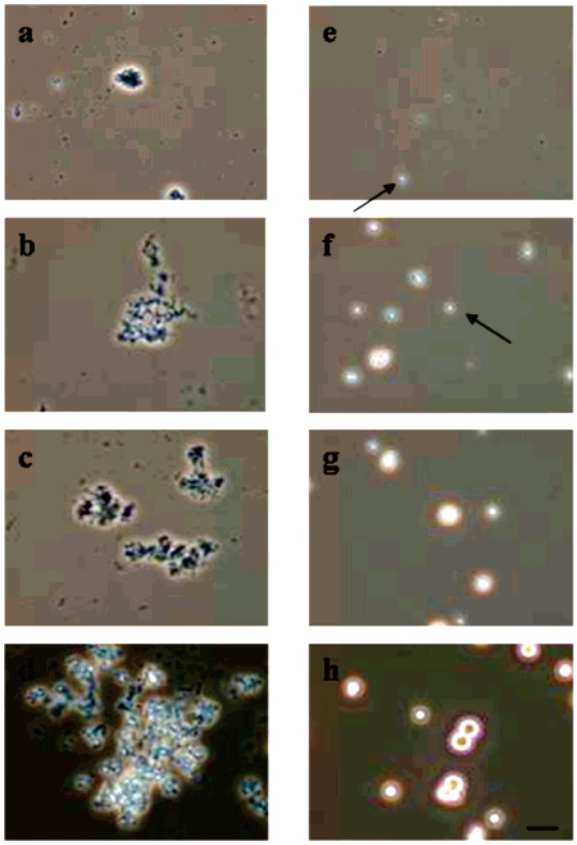

FIGURE 2: Phase contrast micrographs taken at 5 (left) and 45 °C (right) for various LYS/apo α-LA molar ratios: 0.05 (a and e), 0.1 (b and f), 0.2 (c and g), and 1.5 (d and h). Arrows show small coacervates. The scale bar is 10 μm.

Table 1: Size Distribution Parameters of Coacervates Resulting from the Interaction of Apo α-LA with LYS at 45 °C in 30 mM Tris-HCl, 15 mM NaCl Buffer (pH 7.5) and for Different LYS/Apo α-LA Molar Ratios

LYS/apo α-LA molar ratio	*Z* average (nm)	distribution width (nm)
0.05	488 ± 2.8	270
0.1	1123 ± 19	410
0.2	3018 ± 115	810
0.5	3269 ± 148	770
1	5357 ± 32	800
1.5	4820	730

shape, were observed. The size (diameter) of the coacervates depended on the LYS/apo α-LA molar ratio, however, to a lesser extent than that of aggregates observed at 5 °C for the same molar ratio range. The smallest particles were obtained for a molar ratio of 0.05 with diameters of <1 μm (Figure 2e), while the largest particles with diameters of $\sim 3-6$ μm were observed for molar ratios ranging from 0.2 to 2 (Figure 2g,h). For the intermediate molar ratio, the size of coacervates was also intermediate with a diameter of ~ 1 μm (Figure 2f). The coacervates were relatively homogeneous in size for each molar ratio. Coalescence occurring between coacervates to form bigger particles with various morphologies was also visible in Figure 2h. The increase in coacervate size with an increasing LYS/apo α-LA molar ratio was confirmed by dynamic light scattering measurements (Table 1). Moreover, as shown by the increase in the distribution width, the polydispersity of the coacervates slightly increased with an increasing molar ratio. The average sizes deduced from optical microscopy and dynamic light scattering were not affected by dilution of the samples, indicating that coacervates were rather stable to dilution.

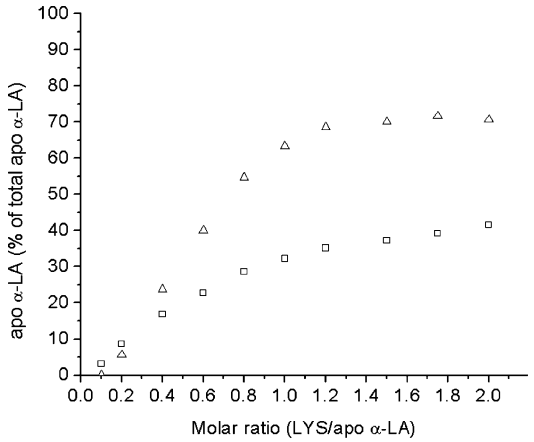

FIGURE 3: Proportion of apo α-LA in the centrifuged material for different LYS/apo α-LA molar ratios at 5 (□) and 45 °C (△). Mixtures of apo α-LA and LYS were centrifuged at 12000*g* for 30 min at 5 or 45 °C. The pellets were washed with 30 mM Tris-HCl, 15 mM NaCl buffer (pH 7.5) and analyzed by rp-HPLC.

The effect of protein concentration on the formation of coacervates was then studied at a LYS/apo α-LA molar ratio of 0.05. It was found that coacervates were formed at a total protein concentration of 1.05 mM. However, their number and size decreased with a decrease in protein concentration until coacervates completely disappeared at a total protein concentration of 0.26 mM (data not shown). The formation and size of coacervates formed at 45 °C were thus dependent on the total concentration of proteins.

Composition of Supramolecular Structures (aggregates versus coacervates). The protein compositions (LYS and apo α-LA) of aggregates and coacervates formed at 5 and 45 °C, respectively, were analyzed by reverse phase HPLC after samples were centrifuged. For all mixtures, analysis of proteins in pellets and supernatants indicated that the initial protein contents were fully recovered. Figure 3 shows the evolution of the apo α-LA fraction in pellets as a function of LYS/apo α-LA molar ratios at 5 and 45 °C. For both temperatures, the apo α-LA fraction in the pelleted material linearly increased at protein molar ratios ranging from 0.1 to 1. For the higher molar ratios, the amount of apo α-LA slightly increased and then tended to reach a plateau value. At plateau values, the apo α-LA fraction in the coacervates (pelleted material collected at 45 °C) was ~2-fold higher than those in the aggregates (pelleted material collected at 5 °C). At a LYS/apo α-LA molar ratio of 2, the proportion of precipitated apo α-LA was 40 ± 4.2% at 5 °C versus 67.8 ± 4.7% at 45 °C. At 45 °C and the lowest protein molar ratio (0.1 LYS/apo α-LA), all apo α-LA was recovered in the supernatant. Consequently, the coacervate-like structures observed for this molar ratio by optical microscopy (Figure 2f) and dynamic light scattering (Table 1) experiments were probably too small to be pelleted under experimental conditions that were used. In other words, the LYS concentration in the mixture is probably too limited to produce structures with a critical size for centrifugation. The amount of apo α-LA in the pellet then increased at higher molar ratios and reached a plateau for a LYS/apo α-LA molar ratio of >1.2. The apo α-LA concentration in solution seemed to be the limiting factor for the formation of coacervates. Figure

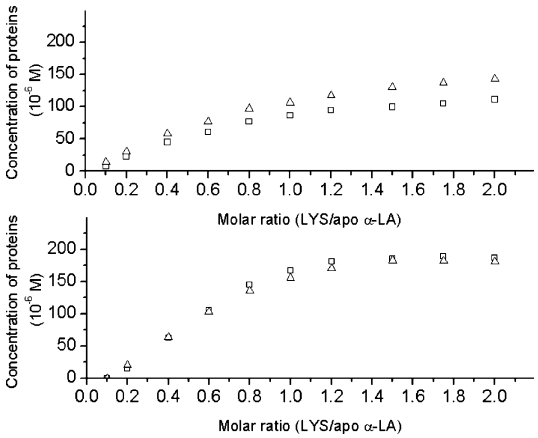

FIGURE 4: Quantity of LYS (Δ) and apo α-LA (□) in the centrifuged material for different (LYS/apo α-LA) molar ratios at 5 (top panel) and 45 °C (bottom panel). Mixtures of apo α-LA and LYS were centrifuged at 12000*g* for 30 min at 5 or 45 °C. The pellets were washed with 30 mM Tris-HCl, 15 mM NaCl buffer (pH 7.5) and analyzed by rp-HPLC.

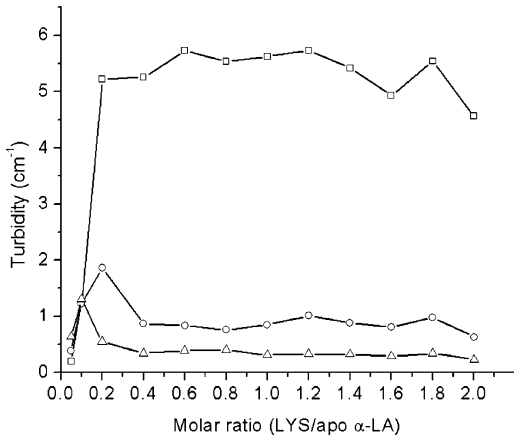

FIGURE 5: Turbidity (cm^{-1}) as a function of LYS/apo α-LA molar ratio in 30 mM Tris-HCl, 15 mM NaCl buffer (pH 7.5) after incubation at 45 °C for (□) 30, (○) 90, and (△) 150 min.

4 reports the recovered insoluble quantity of LYS and apo α-LA at 5 and 45 °C for different protein molar ratios. At 5 °C, the quantity of precipitated LYS was 1.31 ± 0.11-fold higher than that of apo α-LA. At 45 °C, equimolar quantities of both proteins (i.e., molar ratio of 0.97 ± 0.20) were pelleted whatever the initial molar ratio. These results suggest that aggregates and coacervates were different in their relative composition, i.e., protein stoichiometry.

Turbidity of LYS/Apo α-LA Mixtures at 45 °C. Turbidity is a light scattering method that is dependent on the concentration, size, refractive index of scattering particles, and incident wavelength. Turbidity measurements were performed to gain more insight into the supramolecular structures formed at 45 °C. As optical microscopy and dynamic light scattering studies revealed that dilution did not affect the structure of coacervates, samples with a high protein content were diluted before turbidity measurements. The evolution of turbidity as a function of protein molar ratio at three incubation times is shown in Figure 5. After incubation for 30 min, an abrupt increase in turbidity (25-fold) was observed when the LYS/apo α-LA molar ratio increased from 0.05 to 0.2. No further change in turbidity was observed at higher protein molar ratios. Figure 5 also shows that turbidity evolved during storage of samples at

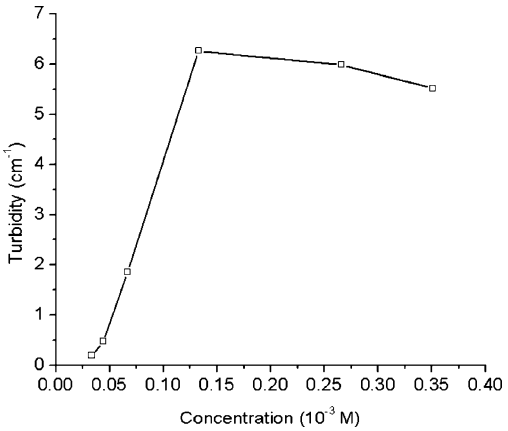

FIGURE 6: Turbidity (cm^{-1}) of LYS/apo α-LA mixtures at 45 °C in 30 mM Tris-HCl, 15 mM NaCl buffer (pH 7.5) as a function of apo α-LA concentration and at a constant LYS/apo α-LA molar ratio of 1.

45 °C. Turbidity of protein mixtures with molar ratios ranging from 0.2 to 2 decreased strongly with an increasing incubation time at 45 °C. Furthermore, a thin layer appeared on the tube walls for longer incubation times. The decrease in turbidity was thus attributed to the formation of this layer throughout a coalescence phenomenon between individual coacervates. The low turbidity values obtained at the lowest protein molar ratio whatever the incubation time at 45 °C would be in agreement with an absence of a coalescence phenomenon.

Turbidity of LYS/apo α-LA mixtures was also measured after incubation for 30 min at 45 °C at various apo α-LA concentrations from 0.033 to 0.351 mM and at a constant protein molar ratio of 1. As shown in Figure 6, an unexpected protein concentration dependence of turbidity is obtained. The turbidity first increased for apo α-LA concentrations ranging from 0.033 to 0.133 mM and then slightly decreased for higher apo α-LA concentrations. The formation and size of coacervates were thus dependent on the total protein concentration in the mixtures.

DISCUSSION

The interaction between LYS and the two structural forms of α-LA was first investigated at 25 °C using isothermal titration calorimetry. ITC is a powerful tool widely used to obtain thermodynamic parameters regarding biological binding processes (*16*−*18*). From our results, it was apparent that LYS did not interact with a native calcium-loaded α-LA form but did interact with calcium-depleted α-LA (apo α-LA). A difference in protein surface charge density associated with Ca^{2+} removal (*19*) may be relevant, initiating an interaction between LYS and α-LA. In fact, three negatively charged residues, Asp82, Asp87, and Asp88, are directly involved in calcium coordination. Hence, removal of calcium leads to a more negatively charged α-LA form that might probably promote the interaction with positively charged LYS. In addition, structural and conformational differences have been reported between holo (folded state) and apo (semifolded states) α-LA (*8*). It was demonstrated, for instance, that, in the absence of calcium at neutral pH and a low ionic strength, α-LA adopts a molten globule-like state (*20*). Consequently, the interaction of apo α-LA with LYS could be promoted throughout the overall con-

formational changes such as higher protein flexibility and surface hydrophobicity induced by Ca^{2+} removal.

The interaction of apo α-LA with LYS characterized by an exothermic signal (Figure 1) was found to be rather complicated, and known models for fitting the ITC signal, to determine the interaction parameters, always failed. Formation of aggregated structures following interaction may explain such an enthalpy change as supported by the presence of precipitated material recovered at the end of titration experiments as well as by turbidity measurements. Indeed, the formation of precipitate was effective at all tested temperatures from 5 to 45 °C. This result is rather surprising and seems to be specific to apo α-LA−LYS interaction. In other protein systems, such as neocarzinostatin−LYS interaction or a mix of two cuticular proteins, protein aggregation was prevented by lowering temperature below 20 °C (*21*, *22*).

Despite the formation of precipitates at low and high temperatures, the shape of calorimetric isotherms differed. Further analysis of the precipitates formed at 5 and 45 °C by optical microscopy showed that supramolecular structures resulting from the interaction between LYS and apo α-LA were different. At 5 °C, aggregates having irregular shapes and disordered structures were formed, while coacervate-like structures with a spherical shape and well-ordered structure were observed at 45 °C (Figure 2). Consequently, the temperature was found to be a key parameter in the formation of the supramolecular structures with respect to the interaction between LYS and apo α-LA. Coacervation is a phenomenon widely spread in the formation of protein−polysaccharide complexes (*23*). Attractive electrostatic interactions between the two (bio)polymers prevail during complex coacervation, a process which is favored by a low temperature and random coil configurations of both biopolymers (*23*). In the case of complex coacervation occurring between weakly charged polyelectrolytes, Ou and Muthukumar (*24*) recently highlighted the fact that complexation was driven by a negative enthalpy due to electrostatic attraction between two oppositely charged chains, with counterion release entropy playing only a minor role. However, the formation of coacervate-type structures is to our knowledge less prevalent in the formation of protein−protein complexes. Coacervation was mainly reported in the case of high-molecular weight proteins such as tropoelastin, legumin, and Tenebrio larval/pupal cuticular proteins (*21*, *25*, *26*). Contrary to what happens in the case of protein−polysaccharide interactions, coacervation is favored with an increasing temperature in the case of protein systems, and the process is said to be entropically driven (*27*, *28*). Accordingly, in our study dealing with protein−protein complexation and coacervation, the formation of coacervate-like structures was favored by an increase in temperature. How do the same binary protein systems lead to completely different structures, i.e., aggregates versus coacervates at 5 and 45 °C, respectively? It is well-known that an increase in temperature may induce an increase in the level of of protein unfolding and gives rise to drastic entropic changes. The denaturation temperature of apo α-LA is around 27 °C, versus 64 °C for holo α-LA (*29*−*31*). This means that, at neutral pH and a low ionic strength, the native structure of apo α-LA is stable at temperature below 27 °C. At 5 °C, global conformational characteristics of apo α-LA were shown to be very similar to those of the native holo form (*32*). At >27 °C, apo α-LA undergoes a conformational change and adopts a molten globule state with a high content of nativelike secondary structure and a lack of specific tertiary structure (*30*, *33*, *34*). Hence, at 5 and 45 °C, apo α-LA exists in two different conformational forms that differ in stability and flexibility. At 45 °C, apo α-LA adopts a more unfolded flexible state with potential hydrophobic domains exposed to the solvent. Hydrophobic interactions certainly play a key role in the coacervation process between LYS and apo α-LA. Moreover, ITC experiments conducted at 45 °C showed a progressive decrease in the magnitude of the interaction signal with an increase in salt concentration until its total disappearance in the presence of 200 mM added NaCl (results not shown). Therefore, if the electrostatic interactions might contribute to the initial recognizance between apo α-LA and LYS, further association and formation of coacervates seem to be mainly driven by protein flexibility and hydrophobic interactions. At 5 °C, apo α-LA adopts a nativelike structure having its hydrophobic domains buried in the core of the molecule and its negatively charged groups no longer involved in the coordination of calcium, more exposed to the solvent. In addition, even if the interaction between the two proteins at 5 °C was suppressed by an increasing ionic strength (results not shown), the observed LYS−apo α-LA aggregation could not be solely attributed to the unique electrostatic interactions resulting from the negatively charged apo α-LA neutralizing the positively charged LYS to reduce the overall entropy of the system. The main driving force in the aggregation could be found in the numerous hydrogen bonds between LYS and apo α-LA preferentially occurring at low temperatures. The decrease in interaction forces through hydrogen bonds would proceed with an increase in temperature, thus favoring the formation of coacervates at 45 °C.

The temperature dependence of the interaction between apo α-LA and LYS, the resulting supramolecular structures, and their evolution are summarized in Figure 7. At 5 °C, the mixture of LYS with apo α-LA gave rise to the formation of polydisperse heterogeneous aggregates. The increase in temperature from 5 to 45 °C affected the stability of the aggregates and led to the formation of coacervates. This temperature dependence assembly is probably linked, in addition to attractive electrostatic interactions, to the conformational change in apo α-LA occurring above 27 °C (a conformational change of LYS in this temperature range being neglected, its denaturation temperature being 74 °C). The observed ability of aggregates formed at 5 °C to be converted to coacervate-like structures at 45 °C underlines a reversible property of these aggregates probably throughout a new balance between involved driven forces (hydrogen, electrostatic, and hydrophobic interactions). The mechanism behind this structural transition is still obscure. Direct mixing of LYS and apo α-LA at 45 °C produced coacervates with equimolar quantities of the two proteins. These coacervates were homogeneous in size in solution with a well-defined structure. Furthermore, the formation and size of coacervates depended on the LYS/apo α-LA molar ratio in the mixtures. The protein molar ratio seems to be a critical factor for the induction and growth of coacervates. At low LYS/apo α-LA molar ratios (<0.2), LYS being the limiting protein as an increase in its concentration seeds the formation of more and

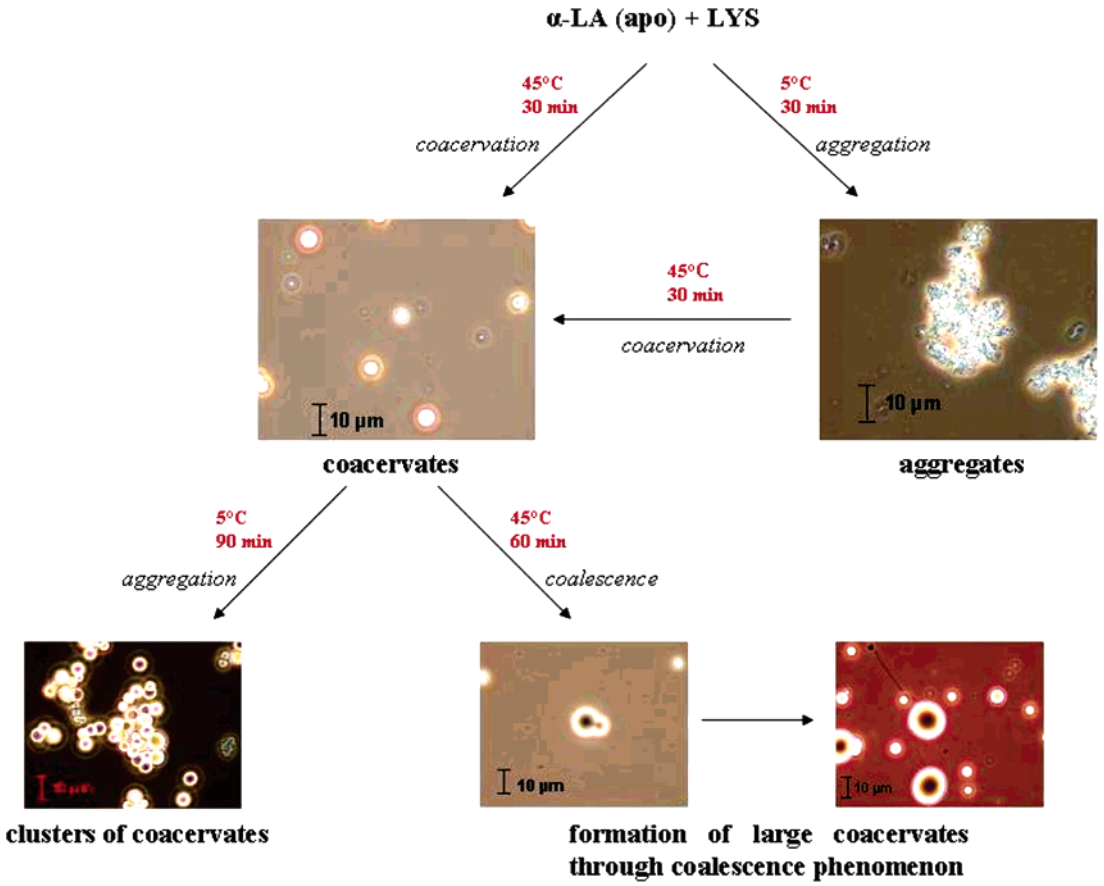

FIGURE 7: Summary of events and formation of supramolecular structures occurring after interaction of apo α-lactalbumin with lysozyme at 5 and 45 °C.

larger cocarvates. In contrast, for protein molar ratios higher than 1, apo α-LA became the limiting component, leading to plateau values for the amount of pelleted proteins and the size of formed structures. In addition, for LYS/apo α-LA molar ratios of <0.2, the coacervates seemed to be stable with aging, while above this ratio, the mixtures exhibited a low stability for prolonged incubation at 45 °C where coalescence phenomena resulting in the formation of larger coacervates occurred. The macroscopic consequence was the formation of a thin layer on the tube walls. On the other hand, the structure of coacervates was stabilized by lowering the temperature from 45 to 5 °C. The decrease in temperature did not involve the structural reorganization of LYS and apo α-LA within coacervates to form aggregates. Furthermore, the decrease in temperature favored the formation of dense networks of coacervate clusters without a detectable coalescence phenomenon. Coacervation has been often reported to be a reversible phenomenon (*28*). The stability and partial irreversibility observed for our system could be explained by the rather specific conditions at a particularly low ionic strength, in which these supramolecular structures are formed.

In this study, the interaction between bovine α-lactalbumin and hen egg white lysozyme was investigated at low ionic strengths and neutral pH. In separate solutions, self-assembly to form fibrils under physicochemical stress conditions, e.g., heat or acidic pH, has been reported for both proteins (*35*, *36*). However, no studies were undertaken to determine the behavior of a mix of these homologous proteins under unstressed conditions with the exception of the work published by Ibrahim et al. (*37*). These authors evidenced the formation of dimeric structures between these two proteins at 25 °C. Our study provides the first detailed demonstration of the association between α-LA and LYS with the following main conclusions. (i) LYS interacts specifically with calcium-depleted α-LA. (ii) LYS−apo α-LA interaction occurs at high (45 °C) and low (5 °C) temperatures and leads to the formation of white precipitates. (iii) Reversible aggregates are formed if apo α-LA is in its native form (5 °C), while coacervate-like structures are obtained with the denatured form of apo α-LA (45 °C). These coacervates can be stabilized toward coalescence at low temperatures. Interaction mechanisms of a variety of structural forms of α-LA with various proteins, including chaperone proteins, start to be well-documented (*20*, *38*). An illustration that subtle heat-induced conformational changes in apo α-lactalbumin affect its type of association with lysozyme and lead to drastic changes in the subsequently formed supramolecular structures is given here.

REFERENCES

1. Qasba, P. K., and Kumar, S. (1997) Molecular divergence of lysozymes and α-lactalbumin, *Crit. Rev. Biochem. Mol. Biol. 32*, 255−306.
2. Greene, L. H., Grobler, J. A., Malinovskii, V. A., Tian, J., Acharya, K. R., and Brew, K. (1999) Stability, activity and flexibility in α-lactalbumin, *Protein Eng. 12*, 581−587.
3. Iyer, L. K., and Qasba, P. K. (1999) Molecular dynamics simulation of α-lactalbumin and calcium binding c-type lysozyme, *Protein Eng. 12*, 129−139.
4. McGuffey, M. K., Epting, K. L., Kelly, R. M., and Foegeding, E. A. (2005) Denaturation and aggregation of three α-lactalbumin preparations at neutral pH, *J. Agric. Food Chem. 53*, 3182−3190.

5. Pike, A. C., Brew, K., and Acharya, K. R. (1996) Crystal structures of guinea-pig, goat and bovine α-lactalbumin highlight the enhanced conformational flexibility of regions that are significant for its action in lactose synthase, *Structure 4*, 691−703.
6. Permyakov, E. A., and Berliner, L. J. (2000) α-Lactalbumin: Structure and function, *FEBS Lett. 473*, 269−274.
7. Chrysina, E. D., Brew, K., and Acharya, K. R. (2000) Crystal structures of apo- and holo-bovine α-lactalbumin at 2.2-Å resolution reveal an effect of calcium on inter-lobe interactions, *J. Biol. Chem. 275*, 37021−37029.
8. Kuwajima, K. (1996) The molten globule state of α-lactalbumin, *FASEB J. 10*, 102−109.
9. Griko, Y. V. (2000) Energetic basis of structural stability in the molten globule state: α-Lactalbumin, *J. Mol. Biol. 297*, 1259−1268.
10. Mizuguchi, M., Nara, M., Kawano, K., and Nitta, K. (1997) FT-IR study of the Ca^{2+}-binding to bovine α-lactalbumin: Relationships between the type of coordination and characteristics of the bands due to the Asp COO- groups in the Ca^{2+}-binding site, *FEBS Lett. 417*, 153−156.
11. Redfield, C., and Dobson, C. M. (1988) Sequential ^{1}H NMR assignments and secondary structure of hen egg white lysozyme in solution, *Biochemistry 27*, 122−136.
12. Shih, P., and Kirsch, J. F. (1995) Design and structural analysis of an engineered thermostable chicken lysozyme, *Protein Sci. 4*, 2063−2072.
13. Shih, P., Holland, D. R., and Kirsch, J. F. (1995) Thermal stability determinants of chicken egg-white lysozyme core mutants: Hydrophobicity, packing volume, and conserved buried water molecules, *Protein Sci. 4*, 2050−2062.
14. Ueda, T., Masumoto, K., Ishibashi, R., So, T., and Imoto, T. (2000) Remarkable thermal stability of doubly intramolecularly cross-linked hen lysozyme, *Protein Eng. 13*, 193−196.
15. Caussin, F., Famelart, M. H., Maubois, J. L., and Bouhallab, S. (2003) Mineral modulation of thermal aggregation and gelation of whey proteins: From *β*-lactoglobulin model system to whey protein isolate, *Lait 83*, 353−364.
16. Campoy, A. V., and Freire, E. (2005) ITC in the post-genomic era...? Priceless, *Biophys. Chem. 115*, 115−124.
17. Schueler-Furman, O., Wang, C., Bradley, P., Misura, K., and Baker, D. (2005) Progress in Modeling of Protein Structures and Interactions, *Science 310*, 638−642.
18. Ladbury, J. E., and Chowdhry, B. Z. (1996) Sensing the heat: The application of isothermal titration calorimetry to thermodynamic studies of biomolecular interactions, *Chem. Biol. 3*, 791−801.
19. Permyakov, S. E., Makhatadze, G. I., Owenius, R., Uversky, V. N., Brooks, C. L., Permyakov, E. A., and Berliner, L. J. (2005) How to improve nature: Study of the electrostatic properties of the surface of α-lactalbumin, *Protein Eng., Des. Sel. 18*, 425−433.
20. Lindner, R. A., Kapur, A., and Carver, J. A. (1997) The interaction of the molecular chaperone, α-crystallin, with molten globule states of bovine α-lactalbumin, *J. Biol. Chem. 272*, 27722−27729.
21. Andersen, S. O. (2002) Characteristic properties of proteins from pre-ecdysial cuticle of larvae and pupae of the mealworm *Tenebrio molitor*, *Insect Biochem. Mol. Biol. 32*, 1077−1087.
22. Nicaise, M., Valerio-Lepiniec, M., Minard, P., and Desmadril, M. (2004) Affinity transfer by CDR grafting on a nonimmunoglobulin scaffold, *Protein Sci. 13*, 1882−1891.
23. Schmitt, C., Sanchez, C., Sobry-Banon, S., and Hardy, J. (1998) Structure and Technofunctional Properties of Protein-Polysaccharide Complexes: A Review, *Crit. Rev. Food Sci. Nutr. 38*, 689−753.
24. Ou, Z., and Muthukumar, M. (2006) Entropy and enthalpy of polyelectrolyte complexation: Langevin dynamics simulations, *J. Chem. Phys. 124*, 154902−154911.
25. Irache, J. M., Bergougnoux, L., Ezpeleta, I., Gueguen, J., and Orecchioni, A. M. (1995) Optimization and in vitro stability of legumin nanoparticles obtained by a coacervation method, *Int. J. Pharm. 126*, 103−109.
26. Muiznieks, L. D., Jensen, S. A., and Weiss, A. S. (2003) Structural changes and facilitated association of tropoelastin, *Arch. Biochem. Biophys. 410*, 317−323.
27. Tamburro, A. M., Bochicchio, B., and Pepe, A. (2005) The dissection of human tropoelastin: From the molecular structure to the self-assembly to the elasticity mechanism, *Pathol. Biol. 53*, 383−389.
28. Clarke, A. W., Arnspang, E. C., Mithieux, S. M., Korkmaz, E., Braet, F., and Weiss, A. S. (2006) Tropoelastin massively associates during coacervation to form quantized protein spheres, *Biochemistry 45*, 9989−9996.
29. Hendrix, T., Griko, Y. V., and Privalov, P. L. (2000) A calorimetric study of the influence of calcium on the stability of bovine α-lactalbumin, *Biophys. Chem. 84*, 27−34.
30. Griko, Y. V., and Remeta, D. P. (1999) Energetics of solvent and ligand-induced conformational changes in α-lactalbumin, *Protein Sci. 8*, 554−561.
31. Veprintsev, D. B., Permyakov, S. E., Permyakov, E. A., Rogov, V. V., Cawthern, K. M., and Berliner, L. J. (1997) Cooperative thermal transitions of bovine and human apo-α-lactalbumins: Evidence for a new intermediate state, *FEBS Lett. 412*, 625−628.
32. Wijesinha-Bettoni, R., Dobson, C. M., and Redfield, C. (2001) Comparison of the structural and dynamical properties of holo and apo bovine α-lactalbumin by NMR spectroscopy, *J. Mol. Biol. 307*, 885−898.
33. Dolgikh, D. A., Gilmanshin, R. I., Brazhnikov, E. V., Bychkova, V. E., Semisotnov, G. V., Venyaminov, S. Y., and Ptitsyn, O. B. (1981) α-Lactalbumin: Compact state with fluctuating tertiary structure? *FEBS Lett. 136*, 311−315.
34. Dolgikh, D. A., Abaturov, L. V., Bolotina, I. A., Brazhnikov, E. V., Bychkova, V. E., Gilmanshin, R. I., Lebedev, Y., Semisotnov, G. V., Tiktopulo, E. I., and Ptitsyn, O. B. (1985) Compact state of a protein molecule with pronounced small-scale mobility: Bovine α-lactalbumin, *Eur. Biophys. J. 13*, 109−121.
35. Goers, J., Permyakov, S. E., Permyakov, E. A., Uversky, V. N., and Fink, A. L. (2002) Conformational prerequisites for α-lactalbumin fibrillation, *Biochemistry 41*, 12546−12551.
36. Arnaudov, L. N., and de Vries, R. (2005) Thermally induced fibrillar aggregation of hen egg white lysozyme, *Biophys. J. 88*, 515−526.
37. Ibrahim, H. R., Taniyama, N., and Aoki, T. (2004) Distinct dimerization between α-lactalbumin and lysozyme exhibiting novel antimicrobial activity against Gram-positive and Gram-negative bacteria, *Lett. Drug Des. Discovery 1*, 101−109.
38. Poon, S., Treweek, T. M., Wilson, M. R., Easterbrook-Smith, S. B., and Carver, J. A. (2002) Clusterin is an extracellular chaperone that specifically interacts with slowly aggregating proteins on their off-folding pathway, *FEBS Lett. 513*, 259−266.

BI062129C